Quantum Mechanical Study of the Nonbonded Forces in Water−Methanol Complexes

Karl N. Kirschner and Robert J. Woods*

Complex Carbohydrate Research Center, 220 Riverbend Road, University of Georgia, Athens, Georgia 30602

Received: December 7, 2000; In Final Form: February 16, 2001

The water−methanol dimer can adopt two possible configurations (WdM or MdW) depending on whether the water or the methanol acts as the hydrogen bond donor. The relative stability between the two configurations is less than 1 kcal/mol, and as a result, this dimer has been a challenging system to investigate using either theoretical or experimental techniques. In this paper, we present a systematic study of the dependence of the geometries, interaction energies, and harmonic frequencies on basis sets and treatment of electron correlation for the two configurations. At the highest theory level, MP2/aug-cc-pVQZ//MP2/aug-cc-pVTZ, interaction energies of −5.72 and −4.95 kcal/mol were determined for the WdM and MdW configurations, respectively, after correcting for basis set superposition error using the Boys−Bernardi counterpoise scheme. Extrapolating to the complete basis set limit resulted in interaction energies of −5.87 for WdM and −5.16 kcal/mol for MdW. The energy difference between the two configurations is larger than the majority of previously reported values, confirming that the WdM complex is preferred, in agreement with experimental observations. The effects that electron correlation have on the geometry were investigated by performing optimization at the MP2(full), MP4, and CCSD levels of theory. The approach trajectories for the formation of each dimer configuration are presented and the importance of these trajectories in the development of parameters for use in classical force fields is discussed.

Introduction

The quantitative description of nonbonded interactions between small polar molecules is a first step toward assessing the significance of these interactions in larger biomolecular systems such as carbohydrates, nucleic acids, and proteins. Thorough analysis of nonbonded forces is particularly important due to the abundance of such interactions as hydrogen bonding in chemical and biological systems. Hydrogen bonding is particularly relevant in the case of carbohydrates, where the molecular conformation depends in part on a balance between the weak forces among the hydroxyl groups within the molecule and those between the carbohydrate and the solvent. As water is the only biologically relevant solvent, an accurate description of water−hydroxyl group interactions is essential for understanding the conformational properties of carbohydrates. However, until now relatively little attention has been given to the forces associated with solvation of these molecules. The smallest molecular system that can be used to model carbohydrate−water interaction is the water−methanol dimer. The water dimer has been extensively investigated by both theoretical and experimental methods, but its simplest one-carbon analogue, the water−methanol dimer, is not as well characterized. In this complex, there are two possible hydrogen bond configurations that depend on whether the water (WdM) or the methanol (MdW) acts as the hydrogen bond donor (Figure 1). In the past decade, theoreticians and experimentalists have become increasingly interested in the water−methanol dimer because of the delicate balance between the repulsive and attractive forces that determine the more stable hydrogen bond configuration. Experimentally, both configurations have been observed using infrared matrix isolation.[1,2] Racine and co-workers observed the MdW

configuration in a nitrogen matrix,[1] while in an argon matrix they observed the WdM configuration,[2] indicating that subtle environmental forces can play a role in determining the favored configuration. In vacuo, Huisken and Stemmler, as well as Stockman and co-workers, observed the WdM complex, suggesting that it is the lower energy configuration.[3,4] While the relative stabilities have been qualitatively established, there has yet to be an experimental determination of the interaction energy for either configuration.

Early quantum mechanical studies, performed in 1971 on the two configurations, concluded that MdW is the more stable complex by 1.0 kcal/mol.[5] In contrast, close to a decade later, Tse and co-workers determined at the HF/6-31G(d) level that the WdM configuration was the more stable by 0.2 kcal/mol.[6] In 1998, González and co-workers examined the interaction energies for the two configurations using G2 theory, performed on the MP2/6-311+G(d,p) geometries.[7] They concluded that WdM was the more stable configuration by 0.6 kcal/mol. The following year, Jursic performed a more extensive examination of the two configurations using a variety of theoretical levels and basis sets, but with the interaction energies computed at higher levels than used for the geometry optimizations.[8] In Jursic's study, theory alone was unable to conclusively predict the stability of one configuration over the other because of the disagreements among the various theories and basis sets employed. Only in combination with experimental data could the conclusion be drawn that WdM is the energetically favored configuration.

The inconsistencies between the reported theoretical and experiment results form the grounds for this study. We have undertaken a quantum mechanical investigation of the two water−methanol configurations to provide geometries, harmonic frequencies, and interaction energies that are more rigorous than previously obtained (see Table 1) in hopes of providing a

* Author to whom correspondence should be addressed. Voice: (706) 542-4454. Fax: (706) 542-445. E-mail: rwoods@ccrc.uga.edu.

Non-Bonded Forces in Water−Methanol Complexes

J. Phys. Chem. A, Vol. 105, No. 16, 2001 **4151**
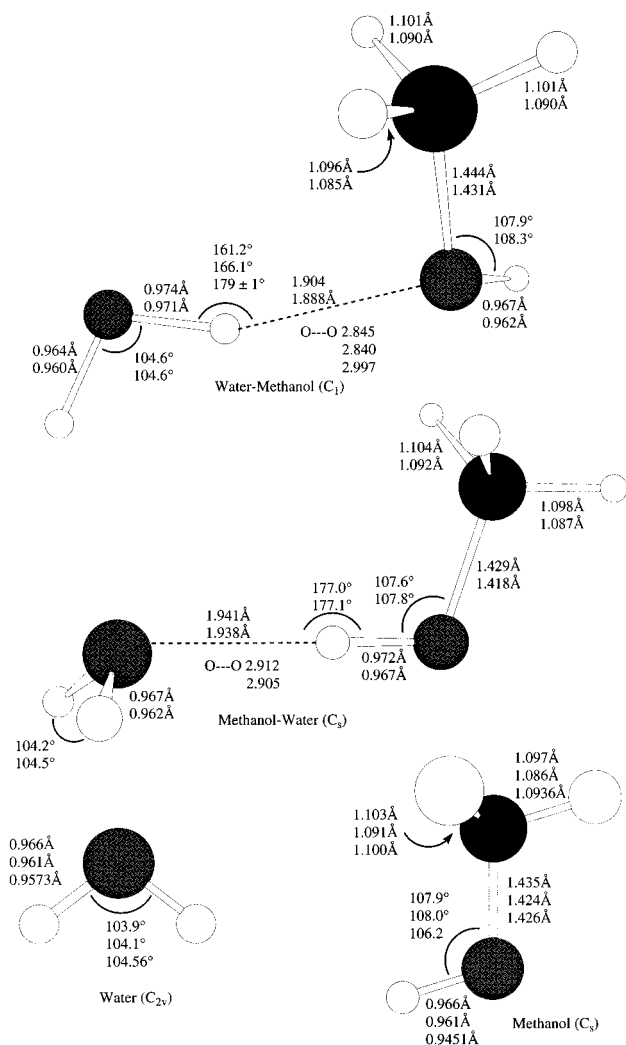
Figure 1. The MP2/aug-cc-pVDZ//MP2/aug-cc-pVDZ (first values), MP2/aug-cc-pVTZ//MP2/aug-cc-pVTZ (second values), and experimental (third values) geometries of WdM, MdW, water, and methanol. Experimental geometries for water and methanol were obtained from refs 21 and 25, respectively.

definitive theoretical treatment of the system. A secondary goal of this work is to provide accurate results that will be implemented in the parametrization of GLYCAM,[9] a parameter set for simulating carbohydrates employing the AMBER[10,11] classical force field. The results from several lower levels of theory were included in this study due to their historic importance in force field parametrization.

Parametrization of the AMBER force field has been done largely using the HF/6-31G(d) level of theory, which has been an adequate level for many of the properties associated with carbohydrates, nucleic acids, and proteins. However, carbohydrates present a unique challenge in parametrization due to the large number of hydroxyl groups that are capable of forming intra- and intermolecular hydrogen bonds. This feature necessitates an increase in the level of quantum accuracy in order to discriminate between the subtle molecular forces present within carbohydrates.

Here, for the first time are presented the approach trajectories for the formation of the WdM and MdW complexes. Full optimization of the dimer configurations yielded geometries and energies that are determined by short-range forces, while the approach trajectories provide an estimation of the strength of long-range forces involved in the formation of the complexes.

In molecular dynamics simulations, accurate descriptions of both the short- and long-range forces, as well as the shape of the potential curves (surfaces), are crucial for reliable molecular simulations. In many biomolecules, the local conformation is determined by short-range interactions, whereas the overall conformational properties (e.g., stability of protein domains) depend on short and long-range interactions. In the case of oligosaccharides both the conformation and dynamics depend on interactions between hydroxyl groups, many of which are separated by distances of over 5 Å. Thus, we are interested not only in the energies of the molecular complexes at the most stable configurations but also at larger separations.

Methodology

Full geometry optimizations of the two hydrogen-bonded configurations and their constituent monomers were performed at the restricted closed shell Hartree−Fock (HF), Møller−Plesset second-order perturbation (MP2),[12] and density functional Becke−Three Lee−Yang−Parr (B3-LYP)[13] levels of theory using the Gaussian94 program suite.[14] All calculations were performed on the closed shell ground electronic state. Only the valence electrons were correlated for the Møller−Plesset theory, except in one instance where both the core and valence electrons were correlated, indicated as MP2(full). A variety of basis sets were used for geometry and energy determination, which included 6-31G(d), 6-31++G(d,p), 6-31++G(2d,2p), and aug-cc-pVxZ (x = D, T, and Q). The most rigorous level employed for determining interaction energies was MP2/aug-cc-pVQZ//MP2/aug-cc-pVTZ. Likewise, the most rigorous geometry optimization was performed at the CCSD/aug-cc-pVDZ level of theory (see Results and Discussion section for further detail). Due to the shallow potential curves of these systems, the keyword OPT=TIGHT was included to increase the convergence criteria in order to obtain reliable geometries. Frequency analyses were performed at appropriate levels of theory, the highest being MP2/aug-cc-pVDZ, to obtain harmonic frequencies and zero-point vibrational energies (ZPVE). The trajectory curves were generated by incrementally adjusting inter-oxygen separations, while allowing the rest of the complex and monomer geometries to relax. Symmetry was maintained during the course of the minimization as appropriate. Interaction energies were determined relative to the fully optimized and isolated monomers (that is, the supermolecule approach). Correction for BSSE was accomplished using the standard Boys−Bernardi functional counterpoise scheme.[15] To be consistent in the sign convention, all stable interaction energies presented in this paper, as well as values taken from the literature, are presented with a negative sign.

Results and Discussion

The relative stabilities between the WdM and MdW complexes are dependent on the subtle balance between repulsive and attractive forces in each configuration. The repulsive forces arise primarily from nuclear−nuclear repulsion and the Pauli exclusion principle. The attractive forces are dominated by electrostatics, with small contributions from induction and dispersion forces. Correct modeling of weak forces is highly dependent on basis set, requiring a good description of the orbital space of the monomers.[16] In the past, a variety of theoretical levels employing small to medium sized basis sets have been used in the hope of determining the lower energy configuration, typically by calculating interaction energies on geometries determined at lower levels of theory.[1,5−8,17−19] While it appears that the growing consensus in the literature is that the WdM

TABLE 1: Ab Initio Results for the Ground State of MdW and WdM

|	$r_e{}^a$	μ^b	energy^c	$D_e{}^d$	$D_o''{}^d$	ZPVE^e	ref
			WdM (C_1)				
HF/6-31G(d)//HF/6-31G(d)	2.952	2.89	−191.0550190	−5.556 (−4.551)	−3.699 (−2.654)	51.000	
HF/aug-cc-pVDZ//HF/aug-cc-pVDZ	2.997	2.92	−191.1105912	−4.124 (−3.941)	−2.405 (−2.222)	50.437	
B3-LYP/6-31++G(d,p)//B3-LYP/6-31++G(d,p)	2.855	2.96	−192.1790691	−6.259 (−5.566)	−4.157 (−3.464)	47.573	
B3-LYP/6-31++G(2d,2p)//HF/6-31G(d)		2.66	−192.1890972	−5.056 (−4.639)			
MP2/6-31G(d)//MP2/6-31G(d)	2.869	1.94	−191.5552944	−7.725 (−4.672)	−5.524 (−2.471)	48.680	
MP2(full)/aug-cc-pVDZ//MP2(full)/aug-cc-pVDZ	2.840	2.10	−191.7009809	−6.296			
MP2/aug-cc-pVDZ//MP2/aug-cc-pVDZ	2.845	2.09	−191.6927353	−6.209 (−5.045)	−4.267 (−3.103)	47.699	
MP2/aug-cc-pVTZ//MP2/aug-cc-pVTZ	2.840	2.53	−191.8675671	−6.003 (−5.514)			
MP2/aug-cc-pVQZ//MP2/aug-cc-pVTZ	2.840	2.52	−191.9243502	−5.867 (−5.717)			
MP2 CBS Limit				−5.87			
HF/STO-3G//HF/STO-3G	2.77			−5.218			5
HF/4-31G (constrained optimization)	2.84	4.48		−8.27			6
HF/6-31G				−7.78			19
HF/6-31G(d) (constrained optimization)	2.97	3.21		−5.73			6
HF/6-31G(d,p)//HF/6-31G(d,p)				−5.433			1
B3-LYP/6-311+G(3df,2p)//B3-LYP/6-311+G(d,p)				−5.9			7
MP2/6-311+G(d,p)//MP2/6-311+G(d,p)	2.906			−6.14			17
MP2/6-311+G(2df,2p)//MP2/6-311+G(d,p)				−5.50			17
MP4/CBSB4//MP2/6-31G(d)				−5.9			8
QCISD(T)/6-311G(d,p)//MP2/6-31G(d′)				−7.2			8
CBSQ				−4.0			8
G2				−3.9			8
G2//MP2(full)6-311+G(d,p)				−5.2			7
Experiment	2.997 ± 0.009	2.625 ± 0.14					4
			MdW (C_s)				
HF/6-31G(d)//HF/6-31G(d)	2.962	2.84	−191.0550728	−5.590 (−4.676)	−3.906 (−2.992)	50.826	
HF/aug-cc-pVDZ//HF/aug-cc-pVDZ	3.039	2.93	−191.1100300	−3.772 (−3.584)	−2.349 (−2.161)	50.141	
B3-LYP/6-31++G(d,p)//B3-LYP/6-31++G(d,p)	2.898	3.02	−192.1781856	−5.705 (−4.873)	−3.909 (−3.077)	47.267	
B3-LYP/6-31++G(2d,2p)//HF/6-31G(d)		2.59	−192.1885096	−4.688 (−4.339)			
MP2/6-31G(d)//MP2/6-31G(d)	2.903	2.45	−191.5548828	−7.467 (−5.268)	−5.639 (−3.440)	48.307	
MP2(full)/aug-cc-pVDZ//MP2(full)/aug-cc-pVDZ	2.906	2.85	−191.6996613	−5.468			
MP2/aug-cc-pVDZ//MP2/aug-cc-pVDZ	2.912	2.85	−191.6914013	−5.372 (−4.480)	−3.789 (−2.897)	47.340	
MP2/aug-cc-pVTZ//MP2/aug-cc-pVTZ	2.904	2.86	−191.8663776	−5.257 (−4.779)			
MP2/aug-cc-pVQZ//MP2/aug-cc-pVTZ		2.86	−191.9231841	−5.135 (−4.946)			
MP2 CBS Limit				−5.16			
HF/STO-3G//HF/STO-3G	2.71			−6.259			5
HF/4-31G (constrained optimization)	2.84	4.13		−7.85			6
HF/6-31G				−6.74			19
HF/6-31G(d) (constrained optimization)	2.97	3.04		−5.55			6
HF/6-31G(d,p)//HF/6-31G(d,p)				−5.517			1
B3-LYP/6-311+G(3df,2p)//B3-LYP/6-311+G(d,p)				−5.2			7
MP2/6-311+G(d,p)//MP2/6-311+G(d,p)	2.855			−6.64			17
MP2/6-311+G(2df,2p)//MP2/6-311+G(d,p)				−6.08			17
MP2/cc-pVDZ (constrained optimization)				−4.08			18
MP2/cc-pVTZ (constrained optimization)				−4.44			18
MP2/cc-pVQZ (constrained optimization)				−4.70			18
MP2/cc-pV5Z (constrained optimization)				−4.80			18
MP2 CBS limit				−4.99			18
MP4/CBSB4//MP2/6-31G(d)				−5.7			8
QCISD(T)/6-311G(d,p)//MP2/6-31G(d′)				−7.2			8
CBSQ				−3.7			8
G2				−3.6			8
G2//MP2(full)6-311+G(d,p)				−4.6			7

^{a} Oxygen−oxygen separation, in angstroms. ^{b} Dipole moment, in Debye. ^{c} Energies are in Hartree. ^{d} Dissociation energies are in kcal/mol, and BSSE-corrected values, in parentheses. ^{e} Zero-point vibrational energies are in kcal/mol.

complex is the more stable configuration, the relative magnitude of its stability remains uncertain.[4,8] Table 1 gives the results from MP2 theory using several augmented and correlation-consistent basis sets. The basis sets appear to converge on an interaction energy for each hydrogen bond configuration (see Figure 2). The MP2/aug-cc-pVQZ//MP2/aug-cc-pVTZ BSSE-corrected interaction energy is −5.72 kcal/mol for the WdM complex and −4.95 kcal/mol for the MdW complex. For comparison purposes, the BSSE-corrected interaction energy for the water dimer is −4.92 kcal/mol at this level of theory. Thus, the WdM complex is more tightly bound than the water dimer, while the MdW complex has essentially the same strength as the water dimer. An approximation to the complete basis set (CBS) limit was accomplished using the exponential function $E_x = E_{CBS} + Be^{-Cx}$, where x is the cardinal number of the basis

set and B and C are adjustable parameters.[20] In this work E_x is the interaction energy obtained using the aug-cc-pVxZ basis sets and E_{CBS} is the interaction energy extrapolated to the complete basis set limit. The BSSE-corrected energies were used for the least-squares-fitting of this equation, since it has been demonstrated that their convergence curves are better behaved then the uncorrected curves.[20] The CBS limit at the MP2 level yielded interaction energies of −5.87 kcal/mol for WdM and −5.16 kcal/mol for MdW. Thus, the WdM complex is the more stable by 0.7 kcal/mol, a larger value than that of 0.3 kcal/mol reported by Jursic.[8]

The geometries of the WdM and MdW complexes, as well as those of their respective monomers, determined at the MP2/aug-cc-pVDZ//MP2/aug-cc-pVDZ and MP2/aug-cc-pVTZ//MP2/aug-cc-pVTZ levels of theory are presented in Figure 1.

Non-Bonded Forces in Water−Methanol Complexes

J. Phys. Chem. A, Vol. 105, No. 16, 2001 **4153**
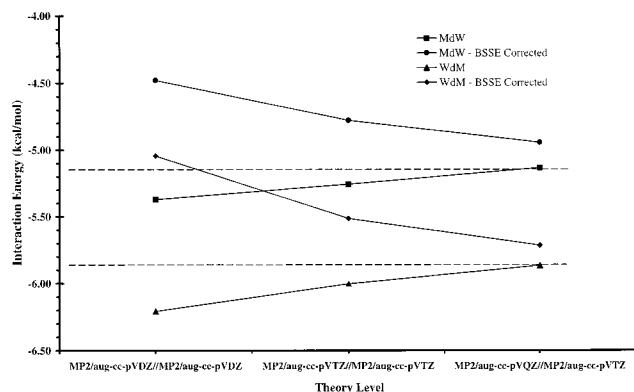
Figure 2. Basis set convergence at the MP2 level of theory for WdM and MdW. Dashed lines indicate the approximate complete basis set limit (see text).

The root-mean-squared (RMS) deviation between the two levels of theory is 0.009 Å for bond lengths and 0.2° for bond angles. The low RMS deviations indicate that the geometries are very close to convergence for the MP2 level of theory. At the MP2/aug-cc-pVTZ//MP2/aug-cc-pVTZ level of theory, the oxygen−oxygen distance in WdM is 2.840 Å, while in MdW a somewhat longer value of 2.904 Å was obtained. Hydrogen bond angles (O−H- - -O) of 166.1° and 177.1° were obtained for WdM and MdW, respectively. Notably, the less stable MdW configuration more closely resembles the water dimer, in terms of hydrogen bond length and angle, with both dimers possessing C_s symmetry. Using microwave spectroscopy for the water−methanol system, Suenram and co-workers determined an oxygen−oxygen distance of 2.997 ± 0.009 Å and a hydrogen bond angle of 179 ± 1°, which they attributed to the WdM configuration.[4] The theoretically determined distances and angles for either the MdW or WdM configuration are in poor agreement with these values, despite the rather high level of theory employed. The disagreements between the MP2/aug-cc-pVTZ geometry and the experimental geometry ($\Delta r_{O- - -O}$ = 0.16 Å and $\Delta\theta_{H-bond}$ = 13°) may arise from several sources.

First of all, the MP2 approximation may not be a sufficient treatment of electron correlation. One way to evaluate the performance of our choice of theory is to examine how well the MP2/aug-cc-pVTZ//MP2/aug-cc-pVTZ level of theory, using the same convergence criteria employed for the water−methanol complexes, performs at reproducing the microwave structure of the water dimer. This theoretical level determines a water dimer oxygen−oxygen distance of 2.907 Å. The microwave structure, determined by Odutola and Dyke, has an oxygen−oxygen distance of 2.976 Å.[21] Thus, in the water dimer, the MP2/aug-cc-pVTZ level of theory determines the oxygen−oxygen distance to be 0.07 Å shorter than the experimental distance. Therefore, it appears that approximately half of the 0.16 Å disagreement between the theory and microwave WdM geometry may be attributed to the level of theory used.

Geometry optimization performed with a more complete treatment of electron correlation, such as using MP4 or coupled-cluster methods (CC), with an appropriate basis set, would help answer this question. To investigate the effects of valence electron correlation on the hydrogen-bonded geometries in the Møller−Plesset regime, the internuclear bond distance, angle, and dihedral angles of WdM were optimized at the MP4/aug-cc-pVDZ level of theory. The individual monomer geometries were constrained to the values found in the MP2/aug-cc-pVDZ complex geometries, since it is unlikely they would change significantly. The oxygen−oxygen distance lengthened only by

0.01 Å and the hydrogen bond angle opened up by ∼3°. Therefore, even extending as far as the MP4 level offers little improvement over the MP2 approximation. Further optimizations were then performed to probe the effect that correlating the core and valence electrons has on the geometry of the two complexes, using the MP2(full)/aug-cc-pVDZ//MP2(full)/aug-cc-pVDZ level of theory. Interestingly, including the correlation of the core electrons at the MP2 level of theory shortened the oxygen−oxygen distance by 0.005 Å and the hydrogen bond angle opened up by 0.2° for the WdM complex, relative to the MP2/aug-cc-pVDZ geometry. Similar results were obtained for the MdW complex, indicating that correlation of the core electron does not significantly alter the geometry of the WdM and MdW complexes at the MP2 level of theory. Since increasing the Møller−Plesset level of theory and the inclusion of the core electrons in the correlation does not appear to bring theory into better agreement with the microwave experiment, a more sophisticated treatment such as CC singles and doubles excitations (CCSD) is warranted. A final calculation at the CCSD/aug-cc-pVDZ level was performed in the same manner as the MP4/aug-cc-pVDZ calculation described above. Even at this level of theory, the oxygen−oxygen distance lengthened only to 2.882 Å, while the hydrogen bond angle was reduced to 162.1°. Thus, the CCSD/aug-cc-pVDZ level of theory is in better agreement with the microwave experimental oxygen−oxygen distance but worsens the hydrogen bond angle agreement.

Alternatively, it is possible that there may be an error in the microwave geometry. It would be interesting to see what results would be obtained if the WdM MP2/aug-cc-pVTZ//MP2/aug-cc-pVTZ geometry were used as the initial guess for fitting the microwave data instead of the assumption that the complex would be similar to the water dimer, as was made in the original analysis of the experimental data.[4] If the experimental hydrogen bond angle were closer to the 165° instead of the near linear value that was originally determined, the oxygen−oxygen distance would be expected to shorten, giving better agreement with the theoretically determined values.

Table 2 gives the theoretical and experimental frequencies[1,2,22,23] for the WdM and MdW complexes, as well as those for their constituent monomers. The formation of the dimer creates six vibrational modes that are unique to the complex, whose most notable vibration is best described as an oxygen−oxygen stretch (ν OO). The theoretical ν OO for WdM and MdW are 192 and 163 cm^{-1}, respectively. In WdM the stretch is 29 cm^{-1} higher in frequency than in MdW, which is further indication that WdM is the more tightly bound configuration. While the computed frequencies agree qualitatively with the experimental data, the quantitative agreement between theory and the matrix experiments is poor. This is to be expected due to the harmonic approximation made in the ab initio calculations, and to the absence of matrix effects in these calculations. However, enlightening trends can be observed between the dimers and the monomers. The frequencies of the hydrogen bond acceptor in each complex remain essentially unchanged from their isolated values, indicating little perturbation in the acceptor geometries. When water becomes the proton donor, its frequencies become significantly shifted, exemplified by a ν^{asym} OH red shift of 38 cm^{-1}. Likewise, when methanol is the hydrogen bond donor its frequencies undergo a significant shift, exemplified by an ν OH red shift of 119 cm^{-1}.

The approach trajectories for the formation of the WdM and MdW complexes are presented in Figures 3 and 4. The trajectories were generated with and without BSSE correction

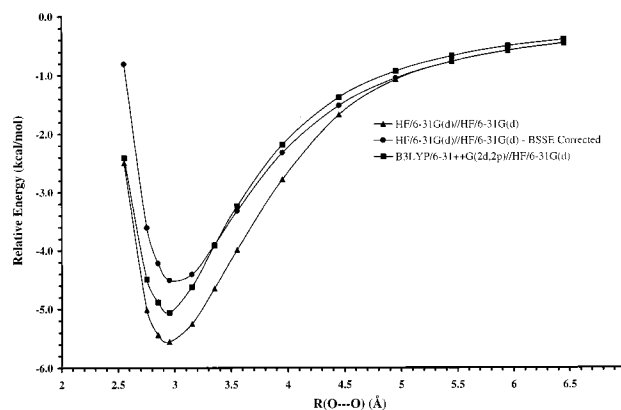**TABLE 2: MP2/Aug-cc-pVDZ and Experimental Frequencies (cm^{-1}) for MdW, WdM, and Their Respective Monomers**

assignment	theoretical	experimental	assignment	theoretical	experiment
WdM			MdW		
ν^{asym} H$_2$O	3900	3703.7[a]	ν^{asym} H$_2$O	3924 (A″)	3713.8[b]
ν OH (methanol)	3828	3663.2	ν^{sym} H$_2$O	3795 (A′)	3627.4
ν^{sym} OH (donor H-water)	3658	3538.7	ν OH (methanol)	3722 (A′)	3536.1
ν^{asym} CH$_3$	3203	3017.8	ν^{sym} CH$_3$	3174 (A′)	2982.4
ν^{asym} CH$_3$	3156	2973.6	ν^{asym} CH$_3$	3112 (A″)	
ν^{sym} CH$_3$	3069		ν^{sym} CH$_3$	3040 (A′)	2835.4
δ H$_2$O	1646	1696.5	δ H$_2$O	1624 (A′)	1600.9
δ^{sym} CH$_3$	1503		δ^{sym} CH$_3$	1507 (A′)	1474.5
δ^{asym} CH$_3$	1493	1466.4	δ^{asym} CH$_3$	1492 (A″)	1463.5
δ^{sym} CH$_3$	1464		δ^{sym} CH$_3$	1463 (A′)	1447.7
δ COH	1364		δ COH	1424 (A′)	1379.6
CH$_3$ wag	1170		CH$_3$ wag	1170 (A″)	
δ CH$_3$ rock + δ COH	1072	1078.0	δ CH$_3$ rock + δ COH	1109 (A′)	1102.9
ν CO	1029	1031.7	v CO	1063 (A′)	1048.3
OH (donor H-water) wag	656		OH(methanol) wag	682 (A″)	606
HOH rock	391		H$_2$O rock	245 (A′)	
OH (methanol) wag	320		H$_2$O twist	188 (A″)	
ν OO	192		ν OO	163 (A′)	
OH(nondonor H-water) wag	124		CH$_3$ twist + H$_2$O wag	84 (A″)	
skeleton deformation	66		skeleton deformation	72 (A″)	
skeleton deformation	58		skeleton deformation	63 (A′)	
CH$_3$OH			H$_2$O		
ν OH	3842 (A′)	3667.0 (3681.5)[c]	ν^{asym} OH	3937.5 (B2)	3942.5[d]
ν^{sym} CH	3190 (A′)	3005.5 (2999.0)	ν^{sym} OH	3803.3 (A1)	3832.2
ν^{asym} CH	3131 (A″)	2961.5 (2970 ± 4)	δ HOH	1622.3 (A1)	1648.5
δ^{sym} HCH	1505 (A′)	1473.0 (avg. 1478)			
δ^{asym} HCH	1494 (A″)	1466.0 (1465 ± 3)			
δ^{sym} HCH	1465 (A′)	1451.5 (1454.5)			
δ COH	1366 (A′)	1334.0 (avg. 1340)			
δ CH$_3$ wag	1169 (A″)	- - - - - (1145 ± 4)			
δ CH rock + δ HOC	1075 (A′)	1076.5 (1074.5)			
ν CO	1044 (A′)	1033.5 (1033.5)			
OH wag	311 (A″)	271.5 - - - - -			

[a] Infrared spectra obtained in an argon matrix, ref 2. [b] Infrared spectra obtained in a nitrogen matrix, ref 1. [c] Infrared spectra obtained in an argon matrix and on gaseous methanol in parentheses, ref 23. [d] Rotational−vibrational spectra of gaseous water, ref 22.
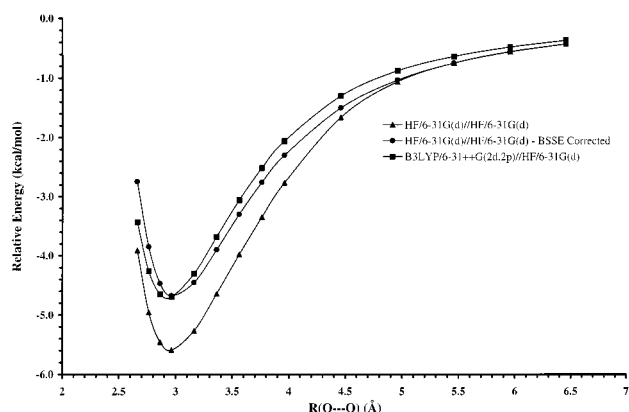
Figure 3. Approach trajectories for WdM computed at HF/6-31G-(d)//HF/6-31G(d), BSSE-corrected HF/6-31G(d)//HF/6-31G(d), and B3-LYP/6-31++G(2d,2p)//HF/6-31G(d) levels of theory.

Figure 4. Approach trajectories for MdW computed at HF/6-31G-(d)//HF/6-31G(d), BSSE-corrected HF/6-31G(d)//HF/6-31G(d), and B3-LYP/6-31++G(2d,2p)//HF/6-31G(d) levels of theory.

at the HF/6-31G(d)//HF/6-31G(d) level of theory. Prior to BSSE correction, the MdW complex is marginally more stable, by 0.03 kcal/mol, than the WdM complex. BSSE correction further enhances its stability, to give a difference in energy favoring the MdW complex by 0.13 kcal/mol (Table 1). Since at higher levels of theory the WdM configuration is favored by as much as 0.7 kcal/mol, neither the BSSE-corrected or uncorrected HF/6-31G(d)//HF/6-31G(d) results reproduce the correct relative stability. Moreover, the BSSE-corrected and uncorrected trajectories for WdM are essentially identical to those for MdW, at the HF/6-31G(d)//HF/6-31G(d) level. This appears to be incorrect since at higher levels of theory the two configurations

become energetically distinguishable, and the approach trajectories for each configuration must also be unique, at least near the minima.

An additional trajectory was calculated using the B3-LYP/6-31++G(2d,2p)//HF/6-31G(d) level of theory. A recent paper by Allinger and co-workers suggests that B3-LYP/6-311++G-(2d,2p)//B3-LYP/6-31G(d,p)5d is an appropriate level of theory for the investigation of carbohydrate properties.[24] They based this proposal on the low magnitude of the BSSE associated with this level in the case of the water dimer. To be as consistent with current AMBER parametrization as possible, we decided to investigate the performance of B3-LYP/6-31++G(2d,2p)

Non-Bonded Forces in Water−Methanol Complexes

J. Phys. Chem. A, Vol. 105, No. 16, 2001 **4155**

energy calculation using the HF/6-31G(d) optimized geometries of the water−methanol complexes. The curves determined by B3-LYP/6-31++G(2d,2p)//HF/6-31G(d,p) behave very differently between the two complexes near the minima. The curve for MdW closely mimics that computed at the BSSE-corrected HF/6-31G(d)//HF/6-31G(d) level (Figure 4), while the curve for WdM differs significantly from the BSSE-corrected Hartree−Fock curve (Figure 3). The B3-LYP data are in better agreement with the rigorous MP2/aug-cc-pVTZ//MP2/aug-cc-pVTZ calculation than the Hartree−Fock data, in that the B3-LYP data correctly predicts the more stable configuration. Prior to BSSE correction, the energy calculated at the B3-LYP level predicts the WdM complex to be the more stable by 0.37 kcal/mol. Performing the BSSE correction at the B3-LYP/6-31++G-(2d,2p) level yields an average BSSE correction of 0.38 kcal/mol for the complexes (Table 1), while leaving the relative stability unchanged. Not surprisingly, it appears that B3-LYP/6-31++G(2d,2p) possesses less BSSE (0.38 kcal/mol versus 0.96 kcal/mol), and is in better agreement with the more rigorous theories, than HF/6-31G(d)//HF/6-31G(d). The HF/6-31G(d)//HF/6-31G(d) level of theory has a difficult time energetically distinguishing between the configurations, while the B3-LYP theory performs qualitatively better. Thus, the approach trajectories calculated by B3-LYP/6-31++G(2d,2p)//HF/6-31G(d) are more reliable than those determined by HF/6-31G(d)//HF/6-31G(d). An interesting trend to note is that at long distances the six curves in Figures 3 and 4 appear to be converging. For example, at 5 Å all curves show that the complexes still possess 1 kcal/mol of stabilization energy. This is significant, considering that there are a large number of interactions that are within 5 Å in carbohydrates and proteins. Correct determination of interaction energies at longer distances is important for correct parametrization of molecular mechanics force fields, such as GLYCAM.

Conclusions

The water−methanol dimer is a challenging system to examine by both theoretical and experimental techniques due to the existence of two possible hydrogen bond configurations, which are very close in energy. Experimentally, both the WdM and MdW configurations have been observed, depending on the chemical environment involved in the experiment. In an attempt to provide a definitive systematic treatment of the system, we have determined the geometries, harmonic frequencies, and BSSE-corrected interaction energies for the WdM and MdW configurations using several levels of theory with basis sets up to Dunning's augmented and correlation-consistent polarized level. At the MP2 complete basis set limit the interaction energies were determined to be −5.87 kcal/mol and −5.16 kcal/mol for WdM and MdW, respectively. Therefore, at the MP2 level the WdM configuration is 0.7 kcal/mol more stable than the MdW configuration, consistent with the experimental data obtained in vacuo. The internuclear separation computed at the MP4/aug-cc-pVDZ and CCSD/aug-cc-pVDZ levels of theory for the WdM configuration are in better agreement with the microwave-determined oxygen−oxygen distance than that computed at the MP2 level. However, at all levels of theory the WdM hydrogen bond angle was computed to be ~165°, which is in disagreement with the experimentally

determined value of 179°. The differences between the theoretical and experimental geometries suggest that further theoretical investigations and possibly a reexamination of the experimental data is warranted.

In addition to these rigorous calculations, we also determined the approach trajectories for WdM and MdW complexes at the HF/6-31G(d)//HF/6-31G(d) (BSSE-corrected and uncorrected) and B3-LYP/6-31++G(2d,2p)//HF/6-31G(d) levels. Both the BSSE-corrected and uncorrected HF/6-31G(d)//HF/6-31G(d) data incorrectly predict the lower energy configuration, compared to the higher levels of theory. In contrast, the B3-LYP/6-31++G(2d,2p)//HF/6-31G(d), which has been suggested as the appropriate level of theory for investigating carbohydrates, correctly predicted WdM to be the more stable configuration, but underestimated the relative stability by approximately 0.4 kcal/mol.

References and Notes

(1) Bakkas, N.; Bouteiller, Y.; Loutellier, A.; Perchard, J. P.; Racine, S. *J. Chem. Phys.* **1993**, *99*, 3335−3342.

(2) Bakkas, N.; Bouteiller, Y.; Loutellier, A.; Perchard, J. P.; Racine, S. *Chem. Phys. Lett.* **1995**, *232*, 90−98.

(3) Huisken, F.; Stemmler, M. *Chem. Phys. Lett.* **1991**, *180*, 332−338.

(4) Stockman, P. A.; Blake, G. A.; Lovas, F. J.; Suenram, R. D. *J. Chem. Phys.* **1997**, *107*, 3782−3790.

(5) Del Bene, J. E. *J. Chem. Phys.* **1971**, *55*, 4633−4636.

(6) Tse, Y. C.; Newton, M.; Allen, L. *Chem. Phys. Lett.* **1980**, *75*, 350−356.

(7) González, L.; Otilla, M.; Yáñez, M. *J. Chem. Phys.* **1998**, *109*, 139−150.

(8) Jursic, B. S. *J. Mol. Struct. (THEOCHEM)* **1999**, *466*, 203−209.

(9) Woods, R. J.; Dwek, R. A.; Edge, C. J.; Fraser-Reid, B. *J. Phys. Chem.* **1995**, *99*, 3832−3846.

(10) Weiner, S. J.; Kollman, P. A.; Case, D. A.; Singh, U. S.; Ghio, C.; Alagona, G.; Profeta, S. J.; Weiner, P. *J. Am. Chem. Soc.* **1984**, *106*, 765−784.

(11) Weiner, S. J.; Kollman, P. A.; Nguyen, D. T.; Case, D. A. *J. Comput. Chem.* **1986**, *7*, 230−252.

(12) Møller, C.; Plesset, M. S. *Phys. Rev.* **1934**, *46*, 618.

(13) Becke, A. D. *J. Chem. Phys.* **1993**, *98*, 5648−5652.

(14) Frisch, M. J.; Trucks, G. W.; Schlegel, H. B.; Gill, P. M. W.; Johnson, B. G.; Robb, M. A.; Cheeseman, J. R.; Keith, T.; Petersson, G. A.; Montgomery, J. A.; Raghavachari, K.; Al-Laham, M. A.; Zakrzewski, V. G.; Ortiz, J. V.; Foresman, J. B.; Cioslowski, J.; Stefanov, B. B.; Nanayakkara, A.; Challacombe, M.; Peng, C. Y.; Ayala, P. Y.; Chen, W.; Wong, M. W.; Andres, J. L.; Replogle, E. S.; Gomperts, R.; Martin, R. L.; Fox, D. L.; Binkley, J. S.; Defrees, D. J.; Baker, J.; Stewart, J. P.; Head-Gordon, M.; Gonzalez, C.; Pople, J. A. *Gaussian 94*, Revision E.2; Gaussian, Inc.: Pittsburgh, PA; 1995.

(15) Boys, S. F.; Bernardi, F. *Mol. Phys.* **1970**, *19*, 553−566.

(16) Chalasinski, G.; Szczesniak, M. M. *Chem. Rev.* **1994**, *94*, 1723−1765.

(17) Masella, M.; Flament, J. P. *J. Chem. Phys.* **1998**, *108*, 7141−7151.

(18) Tsuzuki, S.; Uchimaru, T.; Matsumura, K.; Mikami, M.; Tanabe, K. *J. Chem. Phys.* **1999**, *110*, 11906−11910.

(19) Kim, S.; Jhon, M. S.; Scheraga, H. A. *J. Phys. Chem.* **1988**, *92*, 7216−7223.

(20) van Mourik, T.; Wilson, A. K.; Peterson, K. A.; Woon, D. E.; Dunning, T. H. *Adv. Quantum Chem.* **1999**, *31*, 105−135.

(21) Odutola, J. A.; Dyke, T. R. *J. Chem. Phys.* **1980**, *72*, 5062−5070.

(22) Benedict, W. S.; Gailar, N.; Plyler, E. K. *J. Chem. Phys.* **1956**, *24*, 1139−1165.

(23) Serrallach, A.; Meyer, R.; Günthard, H. H. *J. Mol. Spectrosc.* **1974**, *52*, 94−129.

(24) Lii, J.-H.; Ma, B.; Allinger, N. L. *J. Comput. Chem.* **1999**, *20*, 1593−1603.

(25) Lees, R. M.; Baker, J. G. *J. Chem. Phys.* **1968**, *48*, 5299−5318.